An Absorptive Frequency Selective Reflector With Wide Reflection Band

TIANTIAN GUO [iD], MIN GUO [iD], XUEQING JIA, QIANG CHEN [iD], AND YUNQI FU [iD]
College of Electronic Science, National University of Defense Technology, Changsha 410073, China

Corresponding authors: Min Guo (guomin14@nudt.edu.cn), Qiang Chen (chenqiang08a@nudt.edu.cn), and
Yunqi Fu (yunqifu@nudt.edu.cn)

ABSTRACT In this paper, an absorptive frequency selective Reflector (AFSR) with wide reflection band is proposed. The structure is divided into two layers: a resistive sheet at the top layer, and PEC at the bottom layer, divided by polymethacrylimide (PMI) foam. The resistive sheet layer is composed of a multiple bended strip resonator (MBSR) in the center and two metallic strips loaded with resistors beside MBSR. Two metallic strips loaded with resistors can be equivalent to serial RLC, and the MBSR can be equivalent to parallel LC circuit. The MBSR is mainly used to realize absorption performance beside reflection band and contribute to one of the reflection bands with different resonant modes. The resonant frequencies are adjusted to obtain the wider reflection band. Full-wave simulation results show that the reflection band of the proposed AFSR cover from 8.94 GHz to 15.1 GHz with $|S_{11}| > -1$ dB. The relative bandwidth is 52%. Compared with the earlier reported AFSR, this proposed AFSR owns the widest reflection band and simple structure. In addition, the absorptive bands with $|S_{11}| < -10$ dB are separately located at 3.6 GHz-6.11 GHz and 15.23 GHz - 16.19 GHz. The analysis and the design are presented in this paper. To evaluate the effectiveness of the design, the prototype of the proposed AFSR was fabricated and measured. The measured results are in good agreement with the simulated results.

INDEX TERMS Frequency selection surface, absorptive frequency selection reflector, wide reflection band.

I. INTRODUCTION

Nowadays frequency selective absorbers (FSAs) is one of the hottest topics in electromagnetic field which have lots of applications [1], [2], such as radar cross section (RCS) reduction and interference reduction. To obtain the low RCS, different structures are designed in FSAs which make the electromagnetic wave absorbed by the designed structures. In several applications related to RCS reduction [3], these out of band waves should be absorbed for the bandstop and bandpass cases and the in-band waves should be normally operated. Different from traditional FSAs, the absorptive frequency selective reflector (AFSR) is widely noted which has a reflection band with one- or two-sided absorption bands [4].

The AFSR structures is usually divided into several parts: structures with single or multiple reflection bands, structures that use lumped resistors or commercial absorbers [4]. The AFSR can be used as a ground plane at reflection band, and

can absorb the electromagnetic wave in absorption bands. The antenna can be placed on the AFSR structure to enhance gain in-band and achieve low out of band RCS. The initial way to achieve AFSR structures is to put a bandstop device on top of an absorber [5]. The other way to design an AFSR structure is that the absorption and reflection parts is designed as a unit. These two methods are differentiated by the connection method between the absorption part and the reflection part.

For a stealth target that need to communicate with others in the operation band and be disappeared out of band, that means an AFSR is required here. To effectively transmit electromagnetic wave and reduce object's RCS simultaneously, the work [6] propose a so called band-notched AFSR structure that absorb electromagnetic wave out of band and enhance the radiation characteristic in band. What's more, a reflection structure with two absorption bands at sidebands that joint designed with a mono-pole antenna is proposed which transmit electromagnetic wave in band and absorb electromagnetic wave out of band [7], [8]. This work has

---

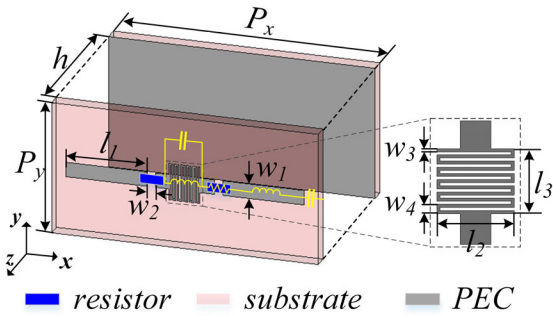The associate editor coordinating the review of this manuscript and approving it for publication was Jaime Laviada [iD].

FIGURE 1. Unit cell of the proposed AFSR structure (with structural parameters: P_x = 18 mm, P_y = 9 mm, h=11 mm, l_1 = 5.5 mm, l_2 = 2.4 mm, l_3 = 2.1 mm, w_1 = 1 mm, w_2 = 0.55 mm, w_3 = 0.1 mm, w_4 = 0.3 mm).

FIGURE 2. The equivalent circuit model of the proposed AFSR structure.

a rather narrow reflection relative bandwidth of 18% which limits its applications. Another single-band AFSR structure, proposed in [5], is based on the 3D FSS concept. This design obtains its reflection band by the short-ended half-wavelength resonator and the open-ended quarter-wavelength resonator. One more design based on the 3D FSS is reported in [9]. This design is based on a wideband absorber with a bandstop FSS layer above. Here, the relative stop-band can be widened to by cascading more bandstop FSS layers to about 15%.

High resolution radars and high capacity communication system with wide operation bandwidth can show high resolution and excellent anti-interference performance [10], [11]. Thus, AFSR with wide reflection bandwidth is required. What's more, the integratable structure is also required to decrease the influence on the appearance as much as possible. Up to now, the maximum relative bandwidth demonstrated in published AFSR works is 22%. However, many applications in radars and communication systems could need a much wider operation bandwidth for improving the range resolution and capacity. Thus, the AFSR with 56% relative bandwidth is designed and analyzed in this paper. The working principle is described and simulated through equivalent circuit models (ECM). The multiple bended strip resonator (MBSR) is introduced in the structure, which generates wide transmission band. With a PEC ground below, the transmission band becomes a reflection band. The half-wavelength space between PEC ground and the MBSR forms a resonator to widen the reflection band. Meanwhile, the resistors beside the MBSR is set to enhance the absorption bands. At last, the prototype is fabricated and measured for an experimental demonstration of the proposed structure.

II. IMPLEMENTATION AND ANALYSIS OF THE AFSR DESIGN

The proposed AFSR structure is shown in Fig. 1. The structure is divided into two layers: a resistive sheet at top layer, and a PEC ground at bottom layer, divided by a polymethacrylimide (PMI) foam. The resistive sheet layer is composed of a multiple bended strip resonator (MBSR) in the center and two metallic strips loaded with resistors beside MBSR. Two layers' structures are separately printed on the
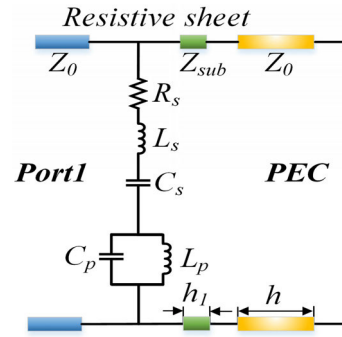
substrate which has a thickness of $h_1 = 0.254$mm, a permittivity of $\varepsilon_r = 3.48$ and a loss tangent of 0.0037.

In this section, we explain the working principle of AFSR. Firstly, as the electromagnetic wave go through the resistive sheet in transmission band, the others will be partly reflected and partly absorbed by the resistive sheet. Then with the ground plane under the resistive sheet, the transmitted electromagnetic wave will be totally reflected by the ground plane. The reflection band can be enhanced by the half-wavelength space resonator. On the other hand, the electromagnetic wave will be absorbed by resistors at two sides of the MBSR [12] on the absorption band.

To clarify the working principle of this proposed AFSR, the multilayer structure can be equivalent to the circuit model shown in Fig. 2. In the equivalent network, the PEC ground is equivalent to a short circuit. The substrate and the PMI foam can be equivalent to transmission lines. h is the thickness of space between substrate and ground. Z_0 indicate the wave impedance of the PMI foam, which is close to wave impedance of free space with 377 Ω. h_1 is the thickness of substrate. Z_{sub} is the wave impedance of the used substrate. The multiple bended strip resonator (MBSR) is equivalent to a parallel LC circuit with inductance L_p and capacitance C_p. L_p is mainly determined by the length of multiple bended strip, and the gap between the bended strips and units contribute to parallel capacitance C_p. L_s and C_s separately denote metal strips' inductance and gap capacitance between units.

To simplify the analysis, the resistive sheet is extracted out from AFSR to discuss separately. According to the ECM, the transmission coefficient of the resistive layer can be expressed as follows:

$$|S_{21}| = \left| \frac{2}{1 + Z_0/Z_{in}} \right| \tag{1}$$

Z_{in} is the impedance of resistive sheet. According to the transmission condition that deduced in works [13], only when Z_{in}/Z_0 is larger than 2 the transmission rate can be higher than 80%. That means the input impedance Z_{in} should be larger than $2Z_0$ if the transmission rate is required to be higher than 80%.

To get a high transmission rate in the transmission band for the resistive sheet which is corresponding to the reflection
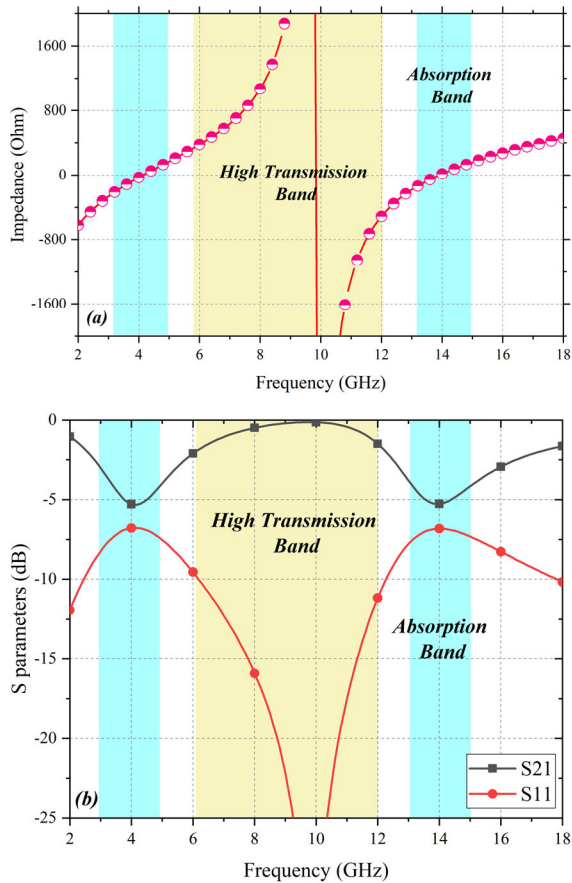
FIGURE 3. The circuit simulated (a) impedance and (b) S parameters of the resistive sheet in AFSR structure.

band for the AFSR structure, the resistive sheet's impedance is well designed to satisfy the high transmission rate condition. The simulated impedance of the resistive sheet is shown in Fig. 3(a). The yellow bands got a high impedance which represent a high transmission rate, and the blue bands got a low impedance which represent a low transmission rate according to the relationship between the impedance and the transmission rate. Fig. 3(b) shows the S parameters corresponding to the resistive sheet in AFSR structure. The high impedance area is in response to the high transmission band, which is in accordance with the analysis above.

Back to the proposed AFSR structure, there are four key resonant frequencies existing, $f_{A1}, f_{A2}, f_{R1}, f_{R2}$. As mentioned before, the impedance should be large to get a high transmission rate. So the zero-point impedance and impedance pole separately contribute to the absorption bands and transmission bands. f_{A1} and f_{A2} representing the two absorption frequencies which are caused by the zero-point impedance. On the other side, f_{R1} representing one of the contributed frequencies in transmission band is decided by impedance pole. The parallel LC circuit can realize impedance pole. So the impedance pole's frequency f_{R1} can be expressed as:

$$f_{R1} = \frac{1}{2\pi\sqrt{L_p C_p}} \qquad (2)$$

To enhance the transmission bandwidth for resistive layer and the reflection bandwidth for AFSR, the bandwidth for f_{R1} and the second contributed frequency f_{R2} is considered. Firstly, the bandwidth for f_{R1}. For the parallel LC circuit, the Q factor can be expressed as follow:

$$Q_p = \frac{1}{\omega_0 L_p} \qquad (3)$$

ω_0 is the central frequency of the operation band. The operation bandwidth can be defined as:

$$BW_p = \frac{f_0}{Q_p} = 2\pi L_p \qquad (4)$$

According to the parallel resonant frequency equation (2), the values of parallel inductance L_p and capacitance C_p determine the parallel resonant central frequency f_{R1} at which the impedance is at pole, and the Q factor or the operation bandwidth is decided by inductance L_p. The reflection coefficient is simulated changing with L_p by ADS, as shown in Fig. 4(b). According to the design in works [14], [15], the bending metal strips is equivalent to parallel inductance. So to enhance transmission band on resistive layer, the structural parameters involving parallel inductance of MBSR should be well optimized.

Secondly, the transmission band contributed frequency f_{R2}. The bottom layer of AFSR is a PEC ground plane. The PMI foam between the top layer and the bottom layer forms a space resonator which contribute to the reflection band in AFSR. The second contributed frequency f_{R2} is decided by the space resonant between resistive sheet layer and PEC ground. With the properly deployed ground plane below, the transmission bands can be changed to reflection bands for a certain frequency f_{R2}. That means that the high transmission rate in resistive sheet layer represent high reflection coefficient in AFSR structure. Combined with the parallel resonant frequency f_{R1}, the transmission bandwidth can be broadened. As described before, beside the impedance poles, the integral multiple wavelength propagation path also contributes to the reflection band in AFSR too. The half-wavelength resonant frequency f_{R2} caused by h-space resonator in AFSR can be expressed as:

$$f_{R2} = \frac{c}{2h\sqrt{\varepsilon}} \qquad (5)$$

h is the height of PMI foam. c is the light speed in vacuum, and ε is the permittivity of PMI which is close to 1.

The reflection coefficient is verified through ADS simulations with the change of the spacer's height h. As we can see in Fig. 4(a), the reflection bandwidth can be enhanced when spacer's height is close to half wavelength $h = 11$ mm.

In this design, the commercial simulation tool CST is also used to analysis the AFSR structure. Two resonant frequencies separately at f_{A1} and f_{A2} are confirmed to achieve absorption bands and f_{R1}, f_{R2} are confirmed to achieve the reflection band in AFSR. The surface current distribution is shown in Fig. 5. As we can see, the MBSR contribute to resonant frequencies with different resonant modes. The
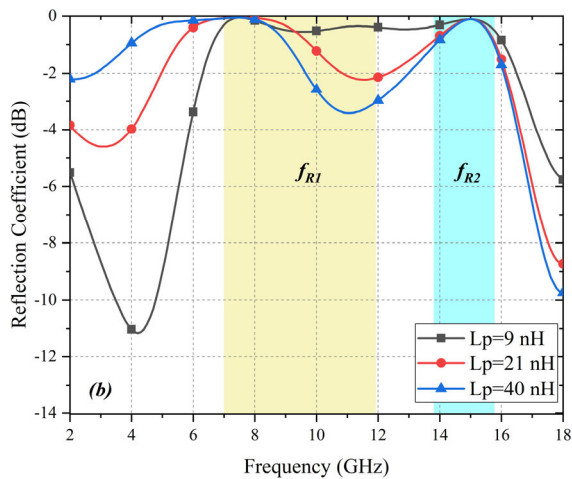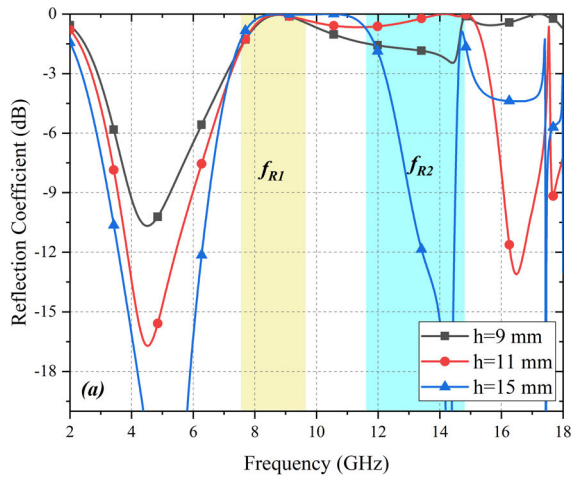
FIGURE 4. The reflection coefficient of AFSR changing with (a) spacer's height h and (b) parallel inductance Lp.

FIGURE 6. Full-wave simulated reflection coefficients of the proposed structure with different incident angles.
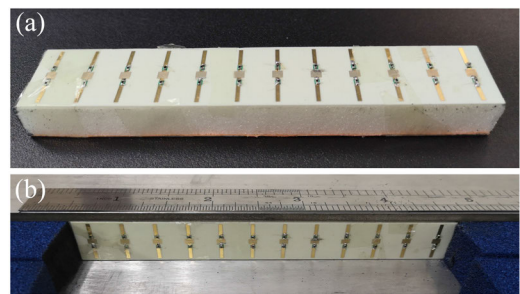
FIGURE 7. Prototype of the AFSR structure. (a) the AFSR (b) measurement setup.
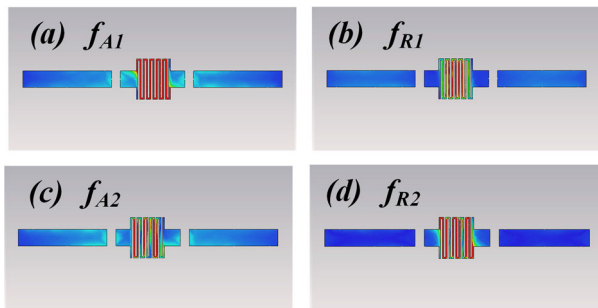

FIGURE 5. Full-wave simulated surface current distribution of the designed AFSR structure at absorption frequencies (a) and (c), and at reflection frequencies (b) and (d).

reflection coefficient on the absorptive resonant frequencies are lower than −15 dB. The reflection band is from 8 GHz to 15.1 GHz. The reflection coefficient is higher than −1 dB in reflection band. Different angles of incident plane wave are also considered in simulations. As shown in Fig. 6, the lower absorption band and the reflection band are insensitive to the incident angle, while the upper absorption band is sensitive
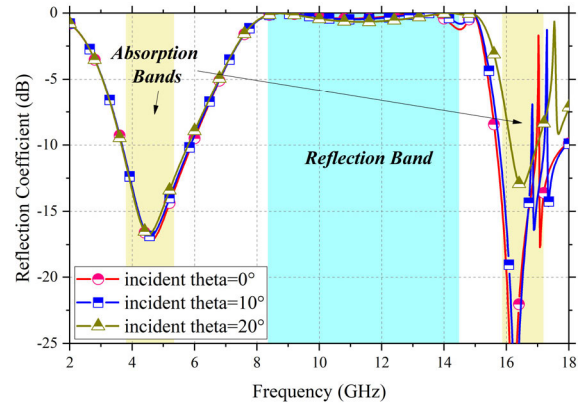
to oblique incidence but within acceptable range. So the proposed structure can be worked at the incident angle between ± 20°.

III. MEASUREMENT RESULTS AND DISCUSSION

To validate the performance of the proposed wideband AFSR structure, the prototype was fabricated and measured in the planar parallel waveguide (PPW). Fig. 7 (a) and (b) show the photograph of the AFSR prototype and the PPW measurement setup which is commonly used in the researches [16]–[18]. The resistive sheet and the ground plane are printed on a dielectric substrate (Rogers 4350B with $\varepsilon_r = 3.48$, thickness of 0.254 mm). The resistors are soldered on the metallic strips. The fabricated AFSR has 1×12 unit cells. The resistive sheet and the ground plane are connected by the PMI foam whose dielectric constant is close to 1.

Fig. 8 shows the comparison of simulated and measured results of the proposed AFSR. Measured results show that the reflection band is from 8.9 GHz to 15.1 GHz. The central frequencies of absorption bands are separately located at 5 GHz and 16 GHz. The measured results are basically in good agreement with the simulated results. The lower boundary of the reflection band is narrowed compared with the simulation results due to the measurement and fabrication errors, such as the rough handmade welding process.
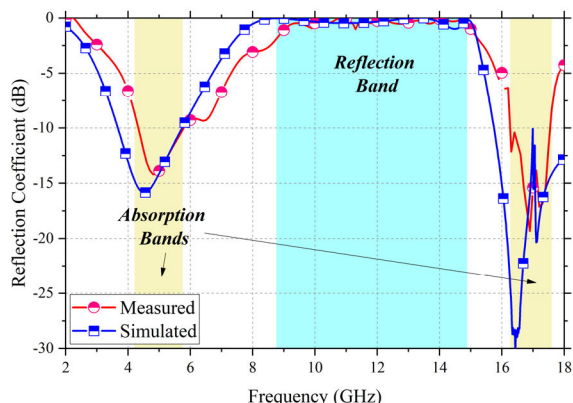
FIGURE 8. Simulated and measured reflection coefficient of the proposed structure.

TABLE 1. Performance comparison of the reported AFSR.

Ref.	Center Frequency	Reflection R.B.	Absorption R.B.	Polarization
[4]	6.5 GHz	15%	4%	Single
[6]	9 GHz	18%	44%	Single
[19]	4.5 GHz	22%	33%	Dual
[20][19]	6 GHz	30%	NA	Dual
This Work	12 GHz	52%	9%	Single

The performance comparison between the proposed AFSR and the other published AFSR are shown in Table 1. Compared with the published works, the proposed AFSR structure in this work has the widest reflection band. However, the performance in this work is achieved only under single polarization. The dual-polarization design will be considered in the next works.

IV. CONCLUSION

The design and analysis of an AFSR structure is demonstrated in this paper. The two resonant frequencies are formed at two sides of the reflection band and the two resonant points should be as far as possible to achieve a wider reflection band. Measured results show that the reflection band is from 8.9 GHz to 15.1 GHz. The absorption bands are separately formed at 4.6 GHz and 16 GHz. The relative bandwidth of the reflection band reaches 52% which is wider than the relative bandwidth of the published works.

REFERENCES

[1] H. Wang, P. Kong, W. Cheng, W. Bao, X. Yu, L. Miao, and J. Jiang, "Broadband tunability of polarization-insensitive absorber based on frequency selective surface," *Sci. Rep.*, vol. 6, Mar. 2016, Art. no. 23081.
[2] F. Costa, A. Monorchio, and G. Manara, "Analysis and design of ultra thin electromagnetic absorbers comprising resistively loaded high impedance surfaces," *IEEE Trans. Antennas Propag.*, vol. 58, no. 5, pp. 1551–1558, May 2010.
[3] Y. Zheng, J. Gao, Y. Zhou, X. Cao, H. Yang, S. Li, and T. Li, "Wideband gain enhancement and RCS reduction of Fabry–Perot resonator antenna with chessboard arranged metamaterial superstrate," *IEEE Trans. Antennas Propag.*, vol. 66, no. 2, pp. 590–599, Feb. 2018.

[4] A. A. Omar, H. Huang, and Z. Shen, "Absorptive frequency-selective reflection/transmission structures: A review and future perspectives," *IEEE Antennas Propag. Mag.*, to be published.
[5] H. Huang, Z. Shen, and A. A. Omar, "3-D absorptive frequency selective reflector for antenna radar cross section reduction," *IEEE Trans. Antennas Propag.*, vol. 65, no. 11, pp. 5908–5917, Nov. 2017.
[6] P. Mei, X. Q. Lin, J. W. Yu, and P. C. Zhang, "A band-notched absorber designed with high notch-band-edge selectivity," *IEEE Trans. Antennas Propag.*, vol. 65, no. 7, pp. 3560–3567, Jul. 2017.
[7] P. Mei, X. Q. Lin, J. W. Yu, P. C. Zhang, and A. Boukarkar, "A low radar cross section and low profile antenna co-designed with absorbent frequency selective radome," *IEEE Trans. Antennas Propag.*, vol. 66, no. 1, pp. 409–413, Jan. 2018.
[8] P. Mei, X. Q. Lin, J. W. Yu, A. Boukarkar, P. C. Zhang, and Z. Q. Yang, "Development of a low radar cross section antenna with band-notched absorber," *IEEE Trans. Antennas Propag.*, vol. 66, no. 2, pp. 582–589, Feb. 2018.
[9] A. A. Omar, Z. Shen, and H. Huang, "Absorptive frequency-selective reflection and transmission structures," *IEEE Trans. Antennas Propag.*, vol. 65, no. 11, pp. 6173–6178, Nov. 2017.
[10] L. Xu, D. Feng, R. Zhang, and X. Wang, "High-resolution range profile deception method based on phase-switched screen," *IEEE Antennas Wireless Propag. Lett.*, vol. 15, pp. 1665–1668, 2016.
[11] B. E. Henty and D. D. Stancil, "Multipath-enabled super-resolution for RF and microwave communication using phase-conjugate arrays," *Phys. Rev. Lett.*, vol. 93, no. 24, 2004, Art. no. 243904.
[12] Y. J. Kim, J. S. Hwang, Y. J. Yoo, B. X. Khuyen, J. Y. Rhee, X. Chen, and Y. Lee, "Ultrathin microwave metamaterial absorber utilizing embedded resistors," *J. Phys. D, Appl. Phys.*, vol. 50, no. 40, Oct. 2017, Art. no. 405110.
[13] Q. Chen, D. Sang, M. Guo, and Y. Fu, "Frequency-selective rasorber with interabsorption band transparent window and interdigital resonator," *IEEE Trans. Antennas Propag.*, vol. 66, no. 8, pp. 4105–4114, Aug. 2018.
[14] Q. Chen, L. Chen, Y. Fu, L. Liu, and J. Bai, "Absorptive frequency selective surface using parallel LC resonance," *Electron. Lett.*, vol. 52, no. 6, pp. 418–419, Mar. 2016.
[15] Q. Chen, S. Yang, J. Bai, and Y. Fu, "Design of absorptive/transmissive frequency-selective surface based on parallel resonance," *IEEE Trans. Antennas Propag.*, vol. 65, no. 9, pp. 4897–4902, Sep. 2017.
[16] M. Guo, Q. Chen, D. Sang, Y. Zheng, and Y. Fu, "Dual-polarized dual-band frequency selective rasorber with low insertion loss," *IEEE Antennas Wireless Propag. Lett.*, vol. 19, no. 1, pp. 148–152, Jan. 2020.
[17] M. Guo, Q. Chen, Z. Sun, D. Sang, and Y. Fu, "Design of dual-band frequency-selective rasorber," *IEEE Antennas Wireless Propag. Lett.*, vol. 18, no. 5, pp. 841–845, May 2019.
[18] M. Guo, Z. Sun, D. Sang, X. Jia, and Y. Fu, "Design of frequency-selective rasorbers based on centrosymmetric bended-strip resonator," *IEEE Access*, vol. 7, pp. 24964–24970, 2019.
[19] Y. Han, L. Zhu, Y. Chang, and B. Li, "Dual-polarized bandpass and band-notched frequency-selective absorbers under multimode resonance," *IEEE Trans. Antennas Propag.*, vol. 66, no. 12, pp. 7449–7454, Dec. 2018.
[20] S. Ghosh and K. V. Srivastava, "Polarization-insensitive single- and broadband switchable absorber/reflector and its realization using a novel biasing technique," *IEEE Trans. Antennas Propag.*, vol. 64, no. 8, pp. 3665–3670, Aug. 2016.

TIANTIAN GUO received the B.Eng. and M.Sc. degrees in electronic engineering from the University of Electronic Science and Technology of China, Chengdu, China, in 2012 and 2015, respectively. She is currently pursuing the Ph.D. degree in microwave and millimeter-wave technology. Her research interests include the design of frequency-selective surface and frequency-selective rasorbers.

MIN GUO received the B.Eng. degree from Xidian University, Xi'an, China, in 2014, and the M.Sc. degree from the National University of Defense Technology, Changsha, China, in 2016, where he is currently pursuing the Ph.D. degree in microwave and millimeter wave technology. His research interests include the design of frequencyselective surface and frequency-selective rasorbers.

QIANG CHEN was born in Henan, China, in 1991. He received the B.Eng., M.Sc., and Ph.D. degrees in electronic science and technology from the National University of Defense Technology, Hunan, China, in 2012, 2014, and 2018, respectively. His current research interests include artificial electromagnetic materials, circuit analog absorbers, and frequency selective surface.

YUNQI FU received the B.Eng., M.Sc., and Ph.D. degrees in electronic science and technology from the National University of Defense Technology, Hunan, China, in 1997, 2000, and 2004, respectively. From 2009 to 2010, he was a Visiting Scholar with The Ohio State University, Columbus, OH, USA. Since 2011, he has been a Professor with the National University of Defense Technology. He has authored or coauthored more than 100 journal articles and three books. He was elected in New Century Talent Supporting Project by Education Ministry, in 2008. He has conducted three NSFC projects and more than ten other projects. His current research interests include artificial electromagnetic metamaterial, microwave and millimeter-wave detection, and imaging. His Ph.D. Dissertation was awarded with the National Excellent Dissertation Nomination Paper and the Provincial Excellent Doctoral Dissertation of Hunan.

XUEQING JIA was born in Tianjin, China, in 1981. He received the B.Eng. and M.Sc. degrees from the National University of Defense Technology, Changsha, China, in 2003 and 2005, respectively, where he is currently pursuing the Ph.D. degree. His current research interests include artificial electromagnetic materials, circuit analog absorbers, and frequency-selective surface.

● ● ●